NanoPhysics Lab Class

Quantum Hall Effect

M2 Quantum, Light, Materials and Nanosciences 2021-2022

Here are few notes concerning the lab class « Quantum Hall Effect ».

1 Theoretical background

1.1 Classical Hall effect

The classical Hall effect was discoverd by Edwin Hall during his PhD in 1879. That is a phenomenon which appears in conductors submitted to magnetic fields. To explain this effect, let us assume for simplicity that we have a two-dimensional electron gas of charge q and mass m forming a ribbon as described in figure 1.

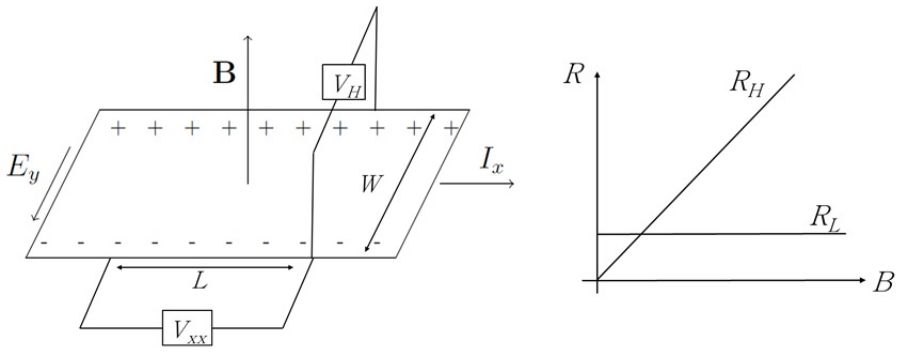

FIGURE 1 – Left : typical geometry for the observation of the Hall effect. A current flows in x-direction, a B-field is applied in z-direction, a Hall voltage arises in y-direction. Right : Longitudinal and transverse resistances evolution with applied magnetic field B.

A simple description of such system is tackled by the Drude model. In such model electrons are classical point particles submitted to a dissipative force $-m\mathbf{v}/\tau$ with τ being the transport scattering time. The electron gas is then submitted to a perpendicular magnetic field $\mathbf{B} = B\mathbf{e_z}$ leading to the equations of motion in the stationnary regime :

$$m\frac{d\mathbf{v}}{dt} = q(\mathbf{E} + \mathbf{v} \times \mathbf{B}) - \mathbf{m}\frac{\mathbf{v}}{\tau} = \mathbf{0}. \tag{1}$$

We now introduce the current density vector $\mathbf{j}= -n_s e\mathbf{v}$ to obtain a matrix relation between the electric field and the current density that generalizes Ohm's law : $\mathbf{E}= \rho\mathbf{j}$ with ρ being the resistivity tensor :

$$\begin{pmatrix} E_x \\ E_y \end{pmatrix} = \rho \begin{pmatrix} j_x \\ j_y \end{pmatrix} = \begin{pmatrix} \rho_{xx} & \rho_{yx} \\ \rho_{xy} & \rho_{yy} \end{pmatrix} \begin{pmatrix} j_x \\ j_y \end{pmatrix} = \begin{pmatrix} 1/\sigma_0 & -B/n_s q \\ B/n_s q & 1/\sigma_0 \end{pmatrix} \begin{pmatrix} j_x \\ j_y \end{pmatrix}. \tag{2}$$

In this equation, $\sigma_0 = n_s q^2\tau/m = n_s q\mu$ is the Drude conductivity at zero field, n_s the charge density and μ the charge carrier mobility. The chosen geometry in figure 1 sets $j_y = 0$ such that one can write the two components of the electric field as :

Julien Basset
Laboratoire de Physique des Solides
julien.basset@universite-paris-saclay.fr

Université Paris–Saclay

$$E_x = \frac{1}{\sigma_0} j_x, E_y = \frac{B}{n_s q} j_x \tag{3}$$

As a result, a flowing current I_x in the x-direction (due to a voltage bias, and thus an electric field in the x-direction) submitted to a perpendicular magnetic field induces an electric field in the y-direction such that a Hall voltage $V_H = WE_y$ appears across the ribbon of width W. Similarly a longitudinal voltage V_{xx} can be measured between two voltage probes separated by a length L and located on the side of the ribbon. With the current I_x defined as $I_x = Wj_x$ one can define the longitudinal R_L and transverse or Hall resistance R_H plotted in figure 1 as :

$$R_L = V_{xx}/I_x = \frac{1}{\sigma_0}\frac{L}{W} = \frac{1}{n_s q \mu}\frac{L}{W}$$
$$R_H = V_H/I_x = \frac{B}{n_s q}$$

From the second equation, we see that if we know the magnetic field, measuring the Hall resistance allows us to access the sign and the density of the charge carriers. Opposingly, if we know the carrier density, one can measure the magnetic field. This is the principle of commercial Hall probes.

Experimental work : density and mobility determination from classical Hall effect - In this labclass, you will have to measure the two resistances at a time. This should allow you to estimate precisely the density n_s and mobility μ of the sample following these two equations :

$$n_s = \frac{1}{q\frac{dR_H}{dB}(B=0)},$$
$$\mu = \frac{\frac{dR_H}{dB}(B=0)}{R_L(B=0)}\frac{L}{W}$$

For typical two-dimensional electron gases made out of n-type GaAs/GaAlAs heterostructures we have $n_s \equiv 1.10^{11} cm^{-2}$ and $\mu \equiv 1.10^6 cm^2.s^{-1}$.

1.2 Shubnikov-de Haas oscillations

Phenomenology - While at low-B the resistivity tensor seems to be rather simple, things get more complicated as the temperature is reduced and the B-field is increased. Indeed, as one increases the B-field, an oscillatory pattern of the longitudinal resistance together with a modulation of the Hall voltage arises. These oscillations have been observed for the first time on three-dimensional Bismuth samples in 1930 by L. Shubnikov and W.J. de Haas and are thus called Shubnikov-de Haas oscillations. This is only in 1966 that Fowler *et al.*[2] demonstrated the same effect in the 2D-case (see for e.g. figure 2).

Quantum interpretation - In order to understand the origin of the Shubnikov-de Haas effect, we have to introduce a quantum treatment of the electrons acting as waves and solve Schrödinger's equation[1]. To do so let us consider the effective mass hamiltonian for a parabolic band :

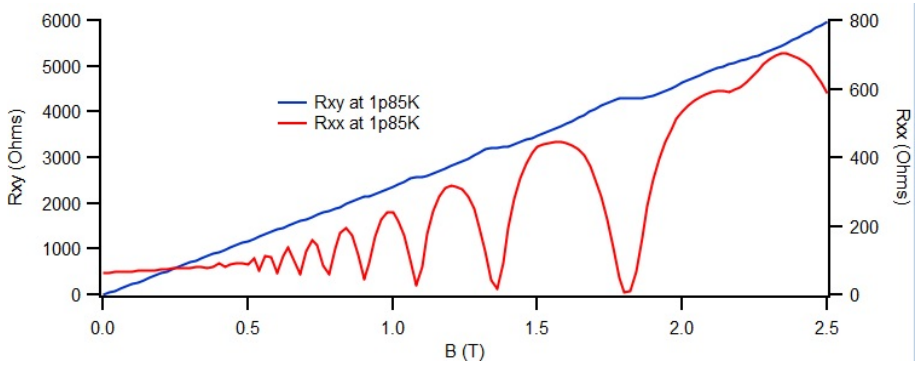

FIGURE 2 – Longitudinal and transverse resistance of a typical GaAs/GaAlAs 2DEG exhibiting SdH oscillations.

$$H = \frac{(\mathbf{p} + e\mathbf{A})^2}{2m^\star} + V(z) \tag{4}$$

where V(z) is the confinement potential in z-direction. For simplicity we choose $\mathbf{A} = (-By, 0, 0)$ describing the magnetic field $\mathbf{B} = (0, 0, B)$. This hamiltonian can be separated in two parts

$$H_z = -\frac{\hbar^2}{2m^\star}\frac{\partial^2}{\partial z^2} + V(z) \tag{5}$$

$$H_{xy} = \frac{(p_x - eB_z y)^2 + p_y^2}{2m^\star}. \tag{6}$$

The first term depends only on the z-coordinate but not on the magnetic field whereas the second one is independent of the confinement potential but depends on B. The eigenvalue problem in the z-direction leads to bound states. In a very thin 2DEG at low temperature, only the lowest of these states is occupied. We say that we are in the quantum limit.

In the plane, the problem can be solved by using the *Ansatz*

$$\psi(x, y) = e^{ik_x x}\eta(y) \tag{7}$$

leading to the eigenvalue problem

$$\left[\frac{p_y^2}{2m^\star} + \frac{1}{2}m^\star\omega_c^2\left(y - \frac{\hbar k_x}{eB_z}\right)^2\right]\eta_{k_x}(y) = E\eta_{k_x}(y). \tag{8}$$

In this equation we have introduced the cyclotron frequency $\omega_c = eB/m^\star$. This is nothing else than a one-dimensional quantum mechanical harmonic oscillator with the k_x-dependent center coordinate $y_0 = \frac{\hbar k_x}{eB}$. As a result the quantized energy states are given by

$$E_n = \hbar\omega_c(n + \frac{1}{2}). \tag{9}$$

Quantum states with different quantum numbers k_x but the same quantum number n are energetically degenerate. They form a so-called *Landau level* [4] as sketched in figure 3.

The energy of a given Landau level increases linearly with the magnetic field B forming the so-called Landau-fan diagram (see figure 3). The degeneracy of a Landau level is given by the requirement that

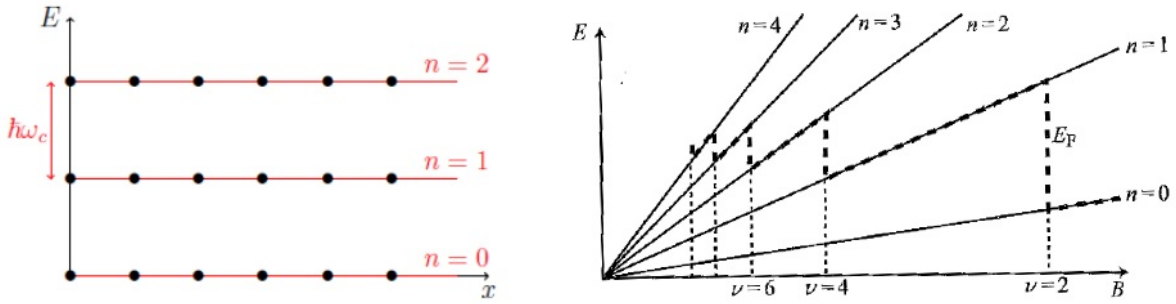

FIGURE 3 – Left : Landau levels separated by the gap energy $\hbar\omega_c$ Right : Landau fan diagram : At high B, all electrons are in the ground state $n = 0$. When decreasing B, the number of available states decreases ($n_l = eB/h$), the filling gets higher. At some point, the number of states in the lowest Landau level is smaller than the electron density. An higher energy states starts to populate. As you lower the field things get periodic with a $1/B$ periodicity.

the center coordinate $y_0 = \frac{\hbar k_x}{eB}$ falls within the width W of the structure, i.e., $0 \leq \frac{\hbar k_x}{eB} \leq W$. As a result the number n_L of allowed k_x states per unit area of the 2DEG is $n_l = eB/h$. If an electron gas has a density n_s, the number $\nu = n_s/n_l$ tells us how many Landau levels are occupied for a specific B-field at $T = O.\nu = hn_s/eB$ is called the filling factor. At a fixed density the Fermi level oscillates as a function of B as shown in figure 3.

Zeeman splitting - In the above considerations, the spin of the electrons was neglected. This is reasonable as long as the Zeeman splitting energy is small compared to the Landau level splitting and broadening. If this is not the case, the Zeeman energy adds to the Landau level energy and we obtain the spectrum

$$E_n^{\pm} = \hbar\omega_c(n + \frac{1}{2}) \pm \frac{1}{2}g^{\star}\mu_B B. \tag{10}$$

In the Landau fan diagram, each Landau level is now split into 2 branches corresponding to spins up and down.

Landau level broadening - Without any disorder, the density of states of a 2DEG submitted to a perpendicular magnetic field is a succession of Dirac peaks located at the energy of the Landau levels

$$D_{2D} = \frac{eB}{h} \sum_{n,\sigma=\pm} \delta(E - E_n^{\sigma}). \tag{11}$$

However, spatial potential fluctuations leads to scattering that lifts the degeneracy of Landau levels. As a result, the ideal delta-shaped density of states peaks are typically broadened by the amount $\hbar/\tau$ related to the mean scattering rate of electrons $1/\tau$ (see figure 1.2). As long as the Landau level spacing is not too high compared to the broadening (see figure 1.2), the density of states demonstrates an oscillatory pattern which in turn leads to an oscillatory magnetoresistance. The exact shape of the broadening is however intimately related to the nature of the dominant scattering processes (long range, short range...).

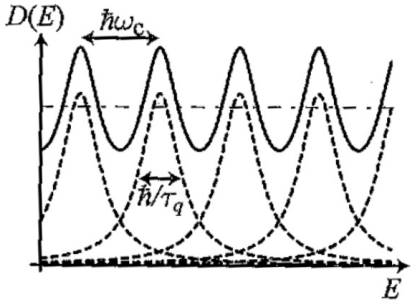

FIGURE 4 – Taken from [1]. Density of states of a 2DEG as a function of energy at finite magnetic fields and finite disorder.

Oscillatory magnetoresistance - The link between density of states and magnetoresistance is in general rather complex. For simplicity, one may assume first that the broadening of the Landau states is Lorentzian and that the magnetic field is not too high. In this situation the density of states can be written as

$$D_{2D}(E,B) = \frac{m^\star}{\pi\hbar^2}\left[1 + \frac{\Delta D}{D}\right] \tag{12}$$

with

$$\frac{\Delta D(E)}{D} = -2exp(-\frac{\pi}{\omega_c\tau})cos(2\pi E/\hbar\omega_c). \tag{13}$$

Further calculations relate the conductance matrix elements to the density of states by equations :

$$\sigma_{xx}(E) = \frac{n_s e^2\tau/m^\star}{1+\omega_c^2\tau^2}\left[1 - \frac{1-\omega_c^2\tau^2}{1+\omega_c^2\tau^2}\frac{\Delta D(E)}{D}\right] \tag{14}$$

$$\sigma_{xy}(E) = \frac{n_s e^2\omega_c\tau^2/m^\star}{1+\omega_c^2\tau^2}\left[\frac{2}{1+\omega_c^2\tau^2}\frac{\Delta D(E)}{D}\right]. \tag{15}$$

From these equations it is immediate that an oscillatory density of states leads to an oscillatory magnetoresistance. This is what are called Shubnikov-deHaas oscillations that should be observed in this labclass.

Experimental work : Electron density extraction from SdH oscillations - It is possible to extract the electron density n_s by using SdH oscillations. Indeed, it can be shown that each minima of the magnetoresistance occurs for $hn/2eB = i + 1/2$, where i is an integer number. By plotting $B_i^{-1} = 2ei/hn_s$ *vs* i one should obtain a straight line with the slope given by $2e/hn_s$. We may also simply watch at the separation of neighboring minima in $1/B$ such that

$$\Delta\left(\frac{1}{B}\right) = \frac{1}{B_{i+1}} - \frac{1}{B_i} = \frac{2e}{hn_s} \tag{16}$$

1.3 Integer quantum Hall effect

Phenomenology - As the magnetic field was further increased, new effects were observed. Indeed, in 1980, Klaus von Klitzing was studying electrical transport in Si-based two-dimensional electron gases [3]. While he was simultaneously measuring R_L and R_H, he observed that at low temperature (T=15K) and

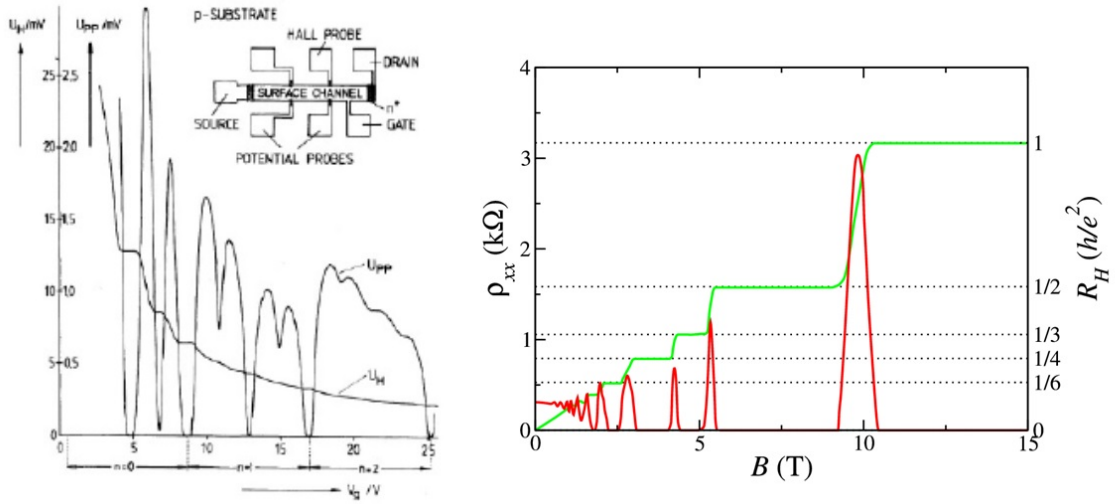

FIGURE 5 – Left : Original measurement of longitudinal and transverse resistances *vs* magnetic field in Si-MOSFET showing the quantum Hall effect as observed by Klitzing in 1980 [3]. Right : A slightly more modern version of the integer quantum Hall effect.

high magnetic field (B=15T), the Hall resistance exhibited plateaus together with a zero-longitudinal resistance (see figure 5).

They further demonstrated that the quantization of the Hall resistance was given by :

$$R_H = \frac{h}{Ne^2} \qquad \text{with } N \text{ an integer number.} \tag{17}$$

The constant $R_K = h/e^2 = 25812.807449\Omega$ is called the von Klitzing constant, or the resistance quantum. This value was found to be independent of the type of materials used. The aim of this labclass is to measure this resistance quantum.

Quantum treatment - The quantum Hall effect is only observed when at high magnetic field the Landau level separation $\hbar\omega_c$ is large compared to the Landau level broadening, i.e., if

$$\hbar\omega_c \gg \hbar/\tau \tag{18}$$
$$\Leftrightarrow \omega_c\tau \gg 1. \tag{19}$$

Clean samples is then a strong prerequisite. Moreover, the thermal broadening k_BT of oscillations in magnetotransport must also be smaller than the Landau gap such that :

$$\hbar\omega_c > k_BT. \tag{20}$$

If these two criteria are fulfilled then one might observe the quantum Hall effect. In this situation, the Landau levels are well separated in energy.

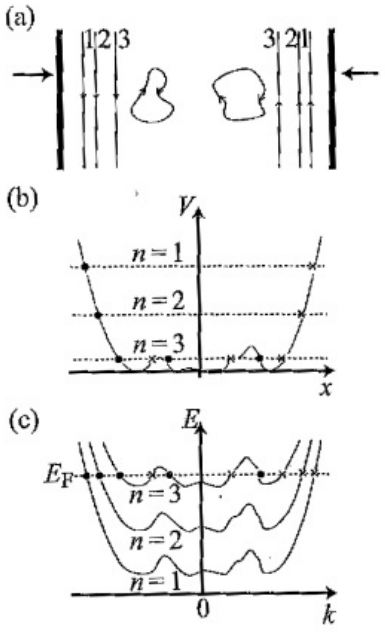

FIGURE 6 – Taken from [1]. Edge states in the quantum Hall regime. (a) Semiclassical electron motion with edge states and localized electrons. (b) Cross sectional view of the Landau states energy in the x-direction. (c) Dispersion relation of the lowest three Landau levels.

Edge states - The bulk energy spectrum previously described cannot explain the quantum Hall effect. In order to explain it we need to consider the finite size of the Hall bars which introduces a confinement potential in the y-direction $V(y)$. The eigenvalue equation then becomes :

$$\left[\frac{p_y^2}{2m^\star} + \frac{1}{2}m^\star\omega_c^2\left(y - \frac{\hbar k_x}{eB_z}\right)^2 + V(y)\right]\eta_{k_x}(y) = E\eta_{k_x}(y) \tag{21}$$

which leads, in the case of weak perturbation, to the eigenenergies :

$$E_n = \hbar\omega_c(n + \frac{1}{2}) + V[\hbar k_x/eB_z]. \tag{22}$$

The potential at the sample edge lifts the Landau level degeneracy and leads to an energy dispersion $E_n(k_x)$ implying a finite group velocity of the states given by $v_x = \frac{1}{\hbar}\frac{\partial V}{\partial k_x}$ which is directed along equipotential lines in the x-direction.

As a result of spatially inhomogeneous potential within the Hall bar and a confinement potential defining the sample edge : in the interior of the sample, the electrons are localized and encircle local extremal points of the potential. At the right edge of the sample (see figure 1.3), spatially separated channels called edge states are formed and move upwards. At the left sample edge, edge states move downwards.

Even if the Fermi energy lies between two Landau levels in the bulk of the sample where all states are localized, extended edge states exist at the sample boundary. Their number corresponds to the filling factor ν or equivalently to the number of intersected Landau levels by the Fermi energy at the edges. All edge states at a particular sample edge have electrons moving in the same direction. Electrons moving in opposite directions are thus spatially separated and backscattering is suppressed. Voltage contacts on the same side of the Hall bar are connected via ideal dissipationless one-dimensional connections. The longitudinal voltage, and with it the longitudinal resistance vanishes. In contrast, if the Fermi level approaches a Landau level, due to disorder, percolating states in the bulk of the sample leads to a finite

resistance. The presence of edge states forms the basis of the description of the quantum Hall effect in the formalism of Landauer and Büttiker [5, 6, 7].

Landauer-Büttiker picture - Let us consider a Hall bar as represented in figure 7 with 6 contacts. When the Fermi energy lies between two Landau levels, bulk states are localized and only edge states propagate to connect neighbouring contacts in clockwise direction.

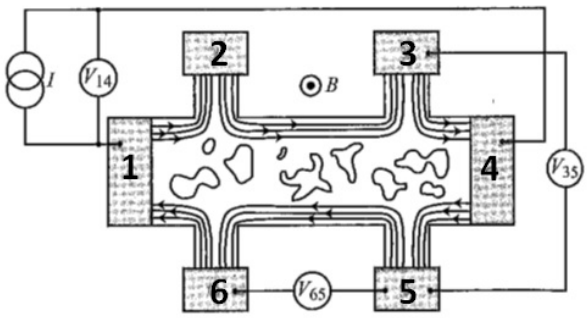

FIGURE 7 – Adapted from [1]. Basic setting allowing to measure and describe the quantum Hall effect in the Landauer-Büttiker formalism. In this picture the filling factor is $\nu = 3$ and disorder induces localized bulk states which do not participate to the transport.

As we have seen in previous paragraph, the transmission from one contact to an other is perfect ($T = 1$) due to the absence of backscattering. In this case, each $1D$ channel biased with a voltage difference V carries a current

$$I_{1D}(V) = \int_{\mu_0}^{\mu_0+eV} e g_{1D}(E) v(E) dE. \tag{23}$$

As in the 1D case the density of states (without spin) is related to the velocity by expression $g_{1D}(E) = 1/hv(E)$ it follows

$$I = \frac{e^2}{h} V = G_0 V. \tag{24}$$

In such circumstances, we say that each perfectly transmitted channel carries the quantum of conductance e^2/h. The number of channels corresponds here to the filling factor ν. For the quantum Hall scenario depicted in figure 7, the transmission matrix then writes :

$$\begin{pmatrix} I_1 \\ I_2 \\ I_3 \\ I_4 \\ I_5 \\ I_6 \end{pmatrix} = \frac{e^2}{h} \begin{pmatrix} \nu & 0 & 0 & 0 & 0 & -\nu \\ -\nu & \nu & 0 & 0 & 0 & 0 \\ 0 & -\nu & \nu & 0 & 0 & 0 \\ 0 & 0 & -\nu & \nu & 0 & 0 \\ 0 & 0 & 0 & -\nu & \nu & 0 \\ 0 & 0 & 0 & 0 & -\nu & \nu \end{pmatrix} \begin{pmatrix} V_1 \\ V_2 \\ V_3 \\ V_4 \\ V_5 \\ V_6 \end{pmatrix}. \tag{25}$$

Experimentally one drives the current from contact 1 to 4 and other contacts only measure voltages. This implies that $I_1 = I$, $I_4 = -I$ and $I_2 = I_3 = I_5 = I_6 = 0$. As a result $V_3 = V_2 = V_1$ and $V_4 = V_5 = V_6$. All contacts on a particular side of the Hall bar are at the same voltage. Mixing these relations, we obtain $I = \nu e^2/h(V_4 - V_1)$. We then define the resistance $R_{ij,kl}$ between contacts i and j with the current driven from k to l. In this case the longitudinal and transverse (or Hall) resistance read :

$$R_L = R_{65,14} = \frac{V_6 - V_5}{I} = 0 \tag{26}$$

$$R_H = R_{26,14} = \frac{V_2 - V_6}{I} = \frac{h}{e^2}\frac{1}{\nu}. \tag{27}$$

We can see from this simple calculation that the assumption about the perfect transmission of edge channels lead to the correct results for both the Hall and the longitudinal resistances.

Experimental work : Resistance quantum measurement - Experimentally you will have to verify the resistance quantization and cancellation with respect to the magnetic field and deduce from it the filling factors corresponding to each plateaus.

1.4 Summary

When a 2DEG is submitted to a magnetic field Landau level forms that are separated in energy by $\hbar\omega_c$. These levels have a density of states which is broadened by the disorder $\hbar/\tau$ (see figure 8). The population of these levels is set by the density of electrons available together with the thermal energy. At low field these Landau levels overlap and lead to an oscillatory pattern of the longitudinal resistance with respect to the B-field. At high field, the Landau levels are well separated in energy such that bulk transport is suppressed between adjacent Landau levels (localized states) and permitted when the Fermi energy reaches the bulk Landau level energy. In addition to bulk transport, the edges see their Landau levels going up to eventually cross the Fermi energy on the sides. Each Landau level crossing the Fermi energy forms an edge state that carries perfectly a quantum of conductance leading to the resistance quantization that one should observe in this labclass.

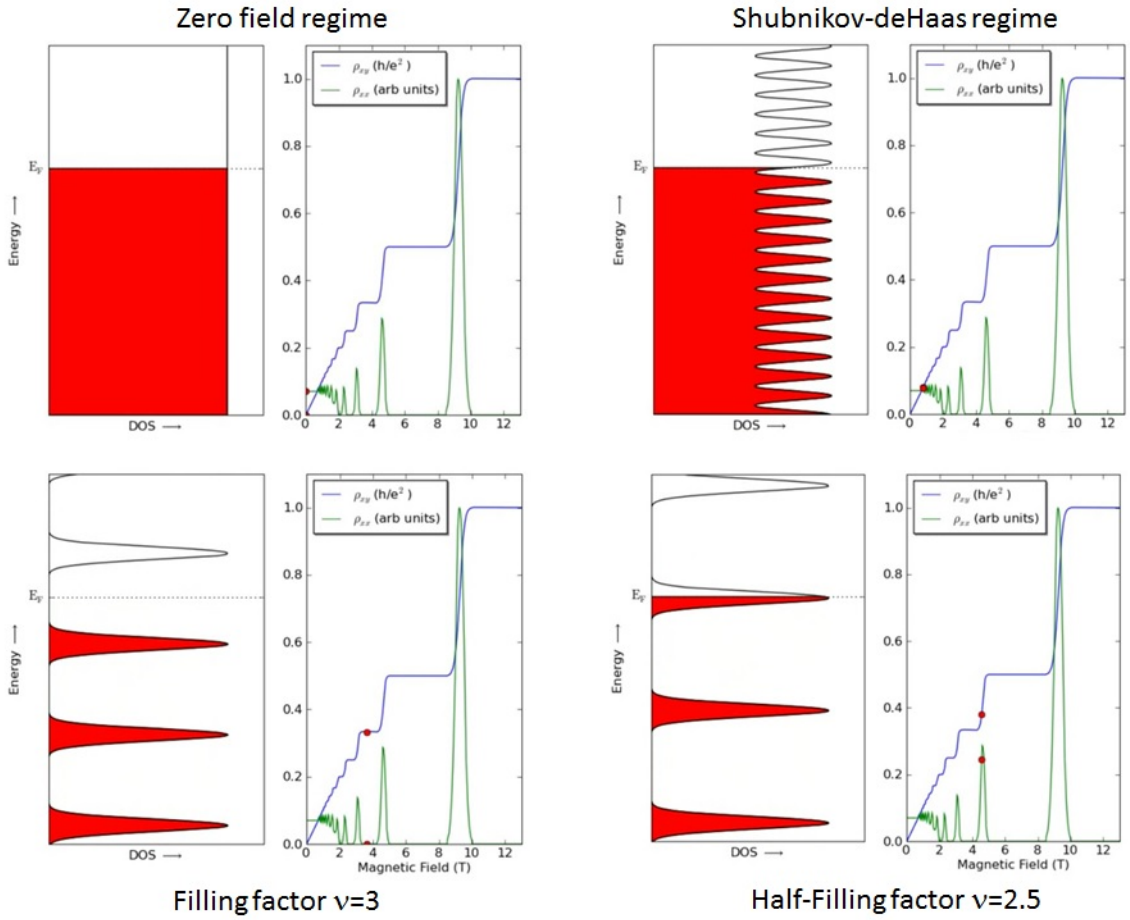

FIGURE 8 – Adapted from [8]. Top left : Bulk density of states of a massive 2DEG at $B = 0$. Top right : Bulk density of states exhibiting non-separated broadened Landau levels as B increases. Bottom left : Well separated bulk Landau levels in the quantum Hall regime with the Fermi energy lying between two levels. Bottom right : Well separated Landau levels in the quantum Hall regime with the Fermi energy lying at the center of a bulk Landau level.

2 Nanofabrication

The Nanofab consists in patterning a Hall bar made out of graphene. The fab starts with some CVD-grown graphene which has been transferred on a doped Silicon wafer using state-of-the-art techniques. The graphene together with the transfer has been realized by the Grenoble research group led by Vincent Bouchiat. The fabrication process used along this practical work is divided in 3 steps.

2.1 Step 1 (optional and to be made by the TA) - Alignment marks

From the bare graphene substrate one makes a first optical lithography of the alignment marks using a negative resist (or AZ5214E in the reverse mode). After revealing, one can evaporate Ti 5nm Au 55 nm and lift-Off with aceton.

2.2 Step 2 - Hallbars patterning and etching

From the sample with alignment marks, we realize an optical lithography (positive resist) step leading to the Hall bar definition. O_2 plasma is used to etch away the graphene followed by an aceton bath to remove the resist.

2.3 Step 3 - Contacting Hallbars

A third optical lithography step is used to define the contacts of the Hallbars (negative resist or AZ5214E in the reverse mode). Evaporation of Ti 5nm Au 100 nm followed by lift-Off in aceton is necessary to finalize the process.

3 Measurement equipment

3.1 Location

The experimental setup of the practical « Quantum Hall effect » is located at the Laboratoire de Physique des Solides (LPS) where a recovery line of Helium is installed.

3.2 Summary

The experiment is rather simple. One has to measure the electrical resistivity or conductivity of a graphene Hall bar at low temperature (4.2K in liquid Helium) as a function of the magnetic field. To this purpose, we have access to the following equipment :

- 100 Liters He Dewar.
- Superconducting coil with maximum field of 5 Teslas at 48.1 A.
- Computer-controlled high current source.
- Dip-stick with sample space and connectors.
- Computer-controlled lock-in amplifiers.
- Voltage amplifiers.
- Low frequency filters.

3.3 He dewar

There are only few dewars that may be used for this experiment. They are the 100 liters with wide collar dewars. Ask Julien Basset or Pascale Auban-Senzier at LPS for ordering. Orders should be placed at least three days in advance.

3.4 Power supply

The current will be supplied to the magnet via a 50A power supply. This power supply is configured in a current controlled mode. The power supply varies the voltage until the target current is achieved. It should be noted that this kind of power supply does not deal well with inductive loads (a superconducting coil is an inductor). To this concern, it is important to sweep slowly the voltage ramp to avoid an overshoot of the current bias which would « quench » the magnet (0.1 A/s at maximum).

The ramp is computer-controlled using a Labview program.

3.5 Magnet insert

The NbTi-based superconducting magnet is suspended in helium by an insert that also guides the dip-stick into the magnet bore. A series of baffles above the magnet prevents room-temperature radiation from reaching the liquid helium. Over-pressure valves are present in case of quench. The specifications of this magnet are listed below :

Rated central field	5.0 T @ 4.2 K
Rated current at 5.0T at 4.2K	48.10 A @ 5.0T
Inductance	0.8 H
Maximum charging rate	0.69 A/s
Field-to-current Ratio	1039.5 Gauss/A
Magnet resistance (at input leads)	496 Ω (at room temperature)

3.6 Dipstick

The dipstick contains resistive wires from room temperature to the He level. These wires are connected at the bottom to a printed circuit board on which is fixed the sample and at the top to a 24 pins vacuum tight Jaeger plug. The sample sits in a vacuum-tight area where He gas acts as an exchange gas during cool down. A breakout-box with standard BNC connectors can be plugged to the Jaeger connector to make the link with standard measurement apparatus (voltage amplifiers and lock-in).

3.7 Voltage and Lock-in amplifiers, filters

In order to realize accurate and precise measurements of the sample resistivity, the experiment provides high quality voltage amplifiers, filters and a lock-in amplifier. The lock-in amplifier of the type SR830 is computer-controlled.

3.8 Computer

The computer will address both the magnetic field current source and the measurement apparatus. It uses Labview and saves data as a .dat file. IgorPro is installed to treat the data.

Références

[1] Thomas Ihn. Semiconductor Nanostructures - Quantum states and electronic transport - Oxford University Press (2011)

[2] Fowler *et al.*, Proc. 8th Int. Conf. Phys. Semicond. (Kyoto) p.331 (1966).

[3] K. v. Klitzing ; G. Dorda ; M. Pepper. New method for high-accuracy determination of the fine-structure constant based on quantized Hall resistance. Phys. Rev. Lett.**45**, 494 (1980).

[4] Landau, L. D. ; and Lifschitz, E. M. ; (1977). Quantum Mechanics : Non-relativistic Theory. Course of Theoretical Physics. Vol. 3 (3rd ed. London : Pergamon Press).

[5] R. Landauer IBM J. Res. Dev. **1**, 223 (1957)

[6] M. Buttiker. Role of quantum coherence in series resistors. Phys. Rev. B **33**, 3020 (1986)

[7] M. Buttiker. Four-Terminal Phase-Coherent Conductance. Phys. Rev. Lett. **57**, 1761 (1986)

[8] `https://en.wikipedia.org/wiki/Quantum_Hall_effect`